

Differentially Coherent Decorrelating Detector for CDMA Single-Path Time-Varying Rayleigh Fading Channels

Huaping Liu and Zoran Siveski, *Member, IEEE*

Abstract—This paper describes a differentially coherent decorrelating detector for a K -user reverse link code-division multiple-access environment that exhibits time-varying Rayleigh fading. The channel is modeled as providing only a single fading path for each user and with no additional means to achieve diversity. The design of the detector is based on using fractionally sampled matched filter outputs to simultaneously achieve two goals: 1) the novel realization of a one shot decorrelator with lower computational complexity and 2) the forming of the maximum-likelihood decision rule on the decorrelated outputs, which results in an effective increase of the correlation in the fading process. Analytical evaluation and simulation of the error probability of the detector demonstrates significant lowering of the error floor in comparison to the decorrelating detector that employs conventional differentially coherent detection.

Index Terms—CDMA, DPSK, decorrelator, multiuser detection, Rayleigh fading.

I. INTRODUCTION

THE common viewpoint of multiuser detection is a joint detection of all the users by exploiting the structure of the multiaccess interference, rather than focusing solely on the desired user and ignoring the rest. The complexity of the optimum multiuser receiver introduced in [1] is, however, exponential in the number of users, which makes it prohibitive in terms of practical implementation. The research efforts that followed were devoted to suboptimum detectors that provide significant improvement over the conventional one, but with a simpler structure that may allow practical realization. An important example of such a receiver is a decorrelating detector [2] with an output that is multiuser interference-free and whose bit-error rate is, therefore, independent of the interfering signals' amplitudes. In addition to its near-far resistance, the decorrelating detector does not require channel estimation. A somewhat inferior, but greatly simplified, form of a decorrelator is introduced in [3], whose processing window is restricted to a bit of interest only (a one-shot decorrelator). A large body of literature on other suboptimum multiuser detectors in the additive white Gaussian noise (AWGN) channel exists, a rather comprehensive survey of which can be found in [4] and [5].

Paper approved by E. S. Sousa, the Editor for CDMA Systems of the IEEE Communications Society. Manuscript received September 29, 1996; revised May 30, 1998. This paper was presented in part at the 30th Annual Conference on Information Sciences and Systems, Princeton, NJ, March 1996.

The authors are with the Wireless Networks Group, Lucent Technologies, Whippany, NJ 07981 USA (e-mail: huapingliu@lucent.com).

Publisher Item Identifier S 0090-6778(99)03315-2.

Realistic wireless multiple-access channels, however, exhibit multipath fading, which is an additional cause of the near-far effect. Multiuser interference in fading channels can significantly degrade the system performance, thereby imposing serious demands on receiver design. Time varying fading channels¹ are especially exacting whenever channel estimation is a necessary part of the detection procedure. The performance limitations of receivers in fading channels are, however, due to inadequate receiver design for such an environment, rather than to the channel itself. Multiuser detection, by alleviating the near-far problem, provides means for improving system performance in mobile channels. An overview of multiuser detection approaches for fading channels is presented in [5].

A decorrelating detector used in conjunction with differentially coherent phase-shift keying (DPSK) modulation does not require channel estimates and seems to be an attractive choice for the multiuser fading environment.² Additionally, the performance analysis of the decorrelator, whose output consists of the desired user and (enhanced) noise only, can be cast into the same analytical framework as a single-user system.

Multiuser detection in the AWGN environment, in which signal energies and phases are unknown to the receiver, is first described in [8]. The resulting DPSK decorrelating receiver is shown to be near-far resistant and to possess a relatively simple structure. The performance of a differentially coherent decorrelating detector in a time-invariant single-path Rayleigh fading channel is investigated in [9]. The effect of fading dynamics on such a receiver is given in [10]. It is shown that the error floor for a differentially coherent decorrelating detector is the same as in the case of a single-user channel.

In this paper we develop the realization of a decorrelating detector in an asynchronous multiuser scenario in which each user's transmission propagates through a single fading path, and no means to achieve improved performance through ex-

¹Often an unquantifiable term, "slow fading," is used when referring to a channel whose gain remains constant over the entire transmission horizon, thus making it perfectly estimable. The terms "fast" or "rapid" fading, then, are used to characterize a channel that does not conform to the above assumption. It appears that time-invariant and time-varying channels are more appropriate respective descriptions (e.g., [6]). The fading rapidity of the latter type can be quantified by an appropriate parameter.

²The results in [7] that compare several multiuser detectors in a single-path Rayleigh fading channels suggest greater robustness of the decorrelator in comparison to more complex detectors that require channel estimates for reconstructing the multiuser interference and, therefore are sensitive to channel estimation errors.

PLICIT diversity, e.g., two antennas, are available. To overcome the imposed limitations, the first step in our approach will be to utilize fractionally sampled matched filter outputs in realizing the computationally efficient, one-shot decorrelator for such a channel³. In a K -user environment, this decorrelator requires the inversion of K matrices of size $K \times K$ only, thus allowing the advantage of parallel processing, and it has a latency of only one bit interval. In [12] it is shown that the error floor in a single-user DPSK transmission can be lowered by applying maximum-likelihood (ML) detection on the vector of multiple samples per symbol interval. We apply the same approach to our already available multisample vector of decorrelated outputs, and, as a result, we achieve a significant reduction in the error floor in comparison to the decorrelating detector used with conventional differentially coherent detection⁴. In addition to the usual requirements for signature sequences and timing of the users, the proposed detector needs only the statistical description of the fading channel, and not the actual realizations of the fading process.

The paper is organized as follows. Section II introduces the received signal model with an associated description of the fading channel. The realization of the decorrelator, the ML detection procedure, and an error probability analysis are presented in Section III. Numerical examples and their interpretations are provided in Section IV, with concluding remarks given in Section V.

II. PRELIMINARIES

Consider K users transmitting asynchronously in a code-division multiple-access (CDMA) mobile environment. Unit energy signature waveform $s_k(t)$, $k = 1, \dots, K$ of duration T , and the chip period T_c is assigned to each user. Differentially encoded bit $d_k(i) \in \{-1, 1\}$ for the i th bit interval of user k with same duration T is obtained from the information bit $b_k(i)$ as $d_k(i) = b_k(i)d_k(i-1)$. The channel for each user is modeled as an independent, narrowband Rayleigh fading channel with multipath spread much shorter than T , which causes only negligible intersymbol interference at the receiver. The channel gain for user k , then, represents multiplicative distortion modeled as a normalized, independent, zero-mean complex-valued wide-sense stationary Gaussian process $c_k(t)$ [13]. The received baseband equivalent complex signal $r(t)$ can, therefore, be expressed as

$$r(t) = \sum_i \sum_{k=1}^K d_k(i) \sqrt{a_k} c_k(t) s_k(t - iT - \tau_k) + n_w(t) \quad (1)$$

where a_k and τ_k are the received energy per bit and relative delay for user k , respectively, and $n_w(t)$ is a zero-mean, complex white Gaussian noise with the one-sided power spectral density N_0 .

³As mentioned in this paper, the one-shot decorrelator for AWGN channel is originally described in [3], and its realization utilizing fractional sampling is presented in [11].

⁴The rationale for making such a comparison is that, as shown in [10], the infinite horizon decorrelator used in conjunction with the conventional (symbol-spaced) differentially coherent detection, has the same error floor as the conventional single user DPSK detector.

For statistical characterization of the fading channel, the space-time correlation function $\Phi(\Delta t)$ is defined as

$$\Phi_k(\Delta t) = E\{c_k(t)c_k^*(t + \Delta t)\}, \quad k = 1, \dots, K \quad (2)$$

where $E\{\cdot\}$ denotes statistical expectations, $*$ denotes conjugate, and $\Phi_k(0) = 1$ due to normalization.

One of the most often used models in the literature for describing the time variations of a channel is a simple, first-order Markov process, which results in the exponential correlation function

$$\Phi_k(\Delta t) = e^{-2\pi f_d T |\Delta t/T|} = \rho^{|\Delta t/T|} \quad (3)$$

where the correlation parameter $\rho = \Phi(T)/\Phi(0)$ determines the fluctuation rate of the fading channel, and f_d represents the maximum Doppler shift. The channel for each user is assumed to fade independently and at the same rate. Another model due to Jakes [14], also referred to as the land-mobile channel model, yields the following correlation function

$$\Phi_k(\Delta t) = J_0(2\pi f_d \Delta t) \quad (4)$$

where $J_0(\cdot)$ is a Bessel function of the first kind. The numerical examples presented in this paper employ both models.

III. MULTIUSER DETECTOR

The proposed multiuser detector, shown in Fig. 1⁵, has a bank of K matched filters as its front end, each filter matched to the user's signature sequence $s_k(t)$. It will be assumed that the time variations of the channel coefficient $c_k(t)$ are such to render the piecewise constant discrete time model approximation valid.

A. Decorrelator

Fractionally sampled matched filter outputs, with relative spacing of the sampling instants coinciding with the users' relative delays⁶, will be used for the realization of the decorrelator. Without loss of generality, we assume that $0 = \tau_1 < \tau_2 < \dots < \tau_K < \tau_{K+1} = T$, and we focus on bit i of user 1 that we, as shown in Fig. 2, position in the interval $[(i-1)T, iT]$. (To simplify notations, the time index will be omitted whenever possible.) We can view each block of time $[\tau_j, \tau_{j+1}]$, $j = 1, \dots, K$ as a K -user synchronous channel with unit-energy waveforms $\bar{s}_k^{(bj)}(t) = s_k^{(bj)}(t)/\sqrt{\epsilon^{(bj)}}$, $k, j = 1, \dots, K$, where

$$s_k^{(bj)}(t) = \begin{cases} s_k(t + \delta_{kj}T - \tau_k), & \tau_j < t < \tau_{j+1} \\ 0, & \text{otherwise} \end{cases}$$

$$\delta_{kj} = \begin{cases} 1 & j < k \\ 0, & \text{otherwise} \end{cases}$$

and

$$\epsilon^{(bj)} = \int_{\tau_j}^{\tau_{j+1}} s_k^2(t + \delta_{kj}T - \tau_k) dt$$

$$= \int_0^T [s_k^{(bj)}(t)]^2 dt, \quad k = 1, \dots, K.$$

In all notations the superscript $^{(bj)}$ denotes block j .

⁵The notations used in the figure are defined in the following sections.

⁶The number of samples per symbol need not be restricted to the number of users K .

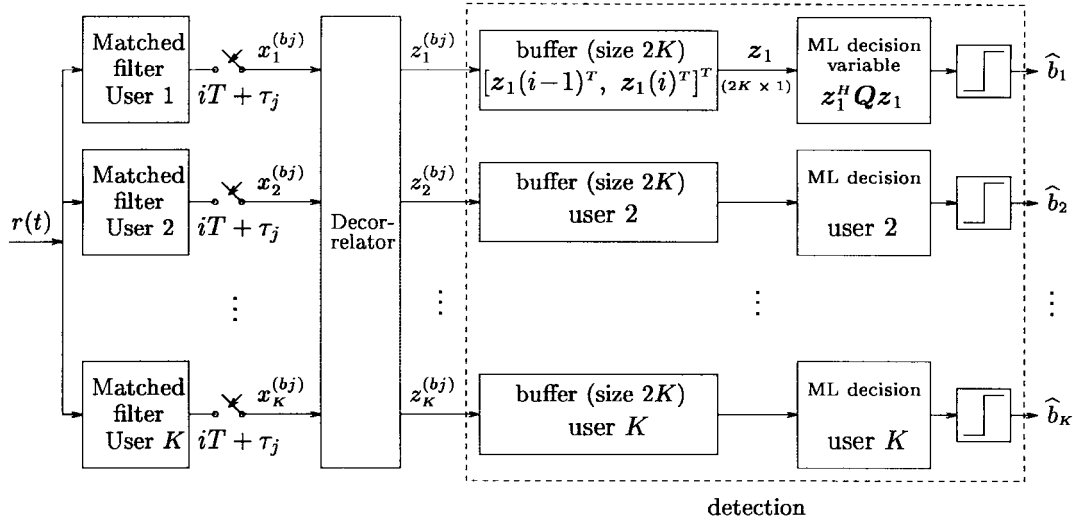
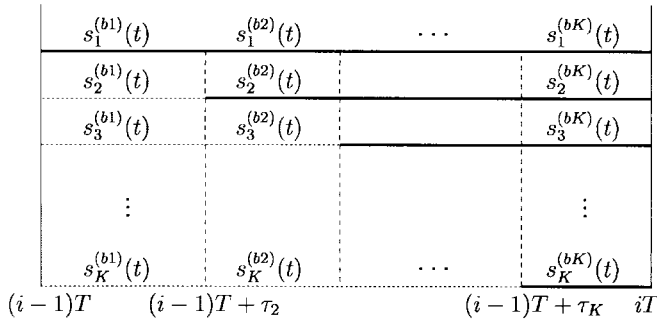


Fig. 1. The proposed multiuser detector.

Fig. 2. Partition of the i th bit interval of user 1 into blocks.

By introducing matrix $\mathbf{P}^{(bj)}$ where the (m, l) th element $p_{ml}^{(bj)}$ is defined as

$$p_{ml}^{(bj)} = \frac{1}{\epsilon^{(bj)}} \int_0^T s_m^{(bj)}(t) s_l^{(bj)}(t) dt, \quad m, l \in (1, \dots, K)$$

the fractionally sampled matched filter output for the j th block in the i th bit interval is⁷

$$\mathbf{x}^{(bj)} = \sqrt{\epsilon^{(bj)}} \mathbf{P}^{(bj)} \mathbf{A} \mathbf{C}^{(bj)} \mathbf{d}^{(bj)} + \mathbf{n}^{(bj)}, \quad j = 1, \dots, K \quad (5)$$

where

$$\begin{aligned} \mathbf{x}^{(bj)} &= [x_1^{(bj)}, x_2^{(bj)}, \dots, x_K^{(bj)}]^T \\ \mathbf{d}^{(bj)} &= [d_1(i), \dots, d_j(i), d_{j+1}(i-1), \dots, d_K(i-1)]^T \\ \mathbf{A} &= \text{diag}[\sqrt{a_1}, \dots, \sqrt{a_K}]. \end{aligned}$$

The additive noise vector for each block, $\mathbf{n}^{(bj)} = [n_1^{(bj)}, \dots, n_K^{(bj)}]^T$, has the covariance matrix $E\{\mathbf{n}^{(bj)} \mathbf{n}^{(bj)H}\} = N_0 \mathbf{P}^{(bj)}$, where H denotes Hermitian transpose.

In the discrete-time channel formulation adopted here, the fading process is piecewise-constant in each block of time⁸

⁷We assume that the channel variations have no effect on the matched filtering operation.

⁸The details of this nonuniform piecewise approximation of channel gains over the interval of duration T are explained in Section IV.

$[\tau_j, \tau_{j+1}]$ so that $\mathbf{C}^{(bj)}$, the matrix of the channel fading coefficients in block j , is given as

$$\begin{aligned} \mathbf{C}^{(bj)} &= \text{diag}[c_1^{(bj)}, \dots, c_K^{(bj)}] \\ &= \text{diag}[c_1(t)|_{t=(i-1)T+\tau_{j+1}}, \dots, c_K(t)|_{t=(i-1)T+\tau_{j+1}}]. \end{aligned} \quad (6)$$

After performing a decorrelating operation on the equivalent K synchronous users in the j th block, the resulting multiuser interference-free vector is

$$\begin{aligned} \mathbf{z}^{(bj)} &= (\mathbf{P}^{(bj)})^{-1} \mathbf{x}^{(bj)} = \sqrt{\epsilon^{(bj)}} \mathbf{A} \mathbf{C}^{(bj)} \mathbf{d}^{(bj)} + \boldsymbol{\xi}^{(bj)}, \\ j &= 1, \dots, K \end{aligned} \quad (7)$$

where

$$\begin{aligned} \mathbf{z}^{(bj)} &= [z_1^{(bj)}, \dots, z_K^{(bj)}]^T \\ \boldsymbol{\xi}^{(bj)} &= [\xi_1^{(bj)}, \dots, \xi_K^{(bj)}]^T \\ &= (\mathbf{P}^{(bj)})^{-1} \mathbf{n}^{(bj)}. \end{aligned}$$

$\boldsymbol{\xi}^{(bj)}$ is the noise vector for all K users in the j th block, and has the covariance matrix

$$E\{\boldsymbol{\xi}^{(bj)} \boldsymbol{\xi}^{(bj)H}\} = N_0 (\mathbf{P}^{(bj)})^{-1}.$$

The decorrelating operation requires an inversion of K matrices of size $K \times K$, which can be done in parallel, and can commence as soon as the vector $\mathbf{x}^{(bj)}$ at the corresponding time instant becomes available.

The $2K$ -sample snapshot of decorrelated outputs in (7) over two adjacent symbol intervals $(i-1)$ and i , which will be used to detect the i th information bit of the desired user⁹, can be written as a $2K \times 1$ vector

$$\begin{aligned} \mathbf{z}_1 &= [z_1^{(b1)}(i-1), \dots, z_1^{(bK)}(i-1), z_1^{(b1)}(i), \dots, z_1^{(bK)}(i)]^T \\ &= [z_1(i-1), z_1(i)]^T \\ &= \sqrt{a_1} \mathbf{D}_1 \mathcal{E}_1 \mathbf{C}_1 + \boldsymbol{\xi}_1 \end{aligned} \quad (8)$$

⁹The decorrelated outputs can be obtained for all K users, but we will, without loss of generality, present a performance analysis only of user 1.

where

$$\begin{aligned} \mathbf{D}_1 &= \text{diag}[\underbrace{d_1(i-1), \dots, d_1(i-1)}_K, \underbrace{d_1(i), \dots, d_1(i)}_K] \\ &= \text{diag}[\mathbf{D}_1(i-1), \mathbf{D}_1(i)] \\ \mathcal{E}_1 &= \text{diag}[\sqrt{\epsilon^{(b1)}}, \dots, \sqrt{\epsilon^{(bK)}}, \sqrt{\epsilon^{(b1)}}, \dots, \sqrt{\epsilon^{(bK)}}] \\ &= \text{diag}[\mathcal{E}_1(i), \mathcal{E}_1(i)] \\ \mathbf{C}_1 &= [c_1^{(b1)}(i-1), \dots, c_1^{(bK)}(i-1), c_1^{(b1)}(i), \dots, c_1^{(bK)}(i)]^T \\ &= [\mathbf{C}_1(i-1)^T, \mathbf{C}_1(i)^T]^T \\ \boldsymbol{\xi}_1 &= [\xi_1^{(b1)}(i-1), \dots, \xi_1^{(bK)}(i-1), \xi_1^{(b1)}(i), \dots, \xi_1^{(bK)}(i)]^T \\ &= [\boldsymbol{\xi}_1(i-1)^T, \boldsymbol{\xi}_1(i)^T]^T. \end{aligned}$$

B. ML Detection on Decorrelator Outputs

Once \mathbf{z}_1 , the multiuser interference-free signal vector over a two-symbol period, is obtained, the detection approach of [12] can be applied. The $2K \times 2K$ covariance matrix of \mathbf{z}_1 in (8) is

$$\begin{aligned} \mathbf{R}_{\mathbf{z}_1} &= E\{\mathbf{z}_1 \mathbf{z}_1^H\} \\ &= E\{a_1 \mathbf{D}_1 \mathcal{E}_1 \mathbf{C}_1 \mathbf{C}_1^H \mathcal{E}_1^H \mathbf{D}_1^H\} + E\{\boldsymbol{\xi}_1 \boldsymbol{\xi}_1^H\} \\ &= a_1 \mathbf{D}_1 \mathcal{E}_1 \mathbf{R}_{\mathbf{c}_1} \mathcal{E}_1^H \mathbf{D}_1^H + \mathbf{R}_{\boldsymbol{\xi}_1} \end{aligned} \quad (9)$$

where

$$\mathbf{R}_{\mathbf{c}_1} = E\{\mathbf{C}_1 \mathbf{C}_1^H\}$$

is the covariance matrix of the fading process at the decorrelator output, and

$$\mathbf{R}_{\boldsymbol{\xi}_1} = E\{\boldsymbol{\xi}_1 \boldsymbol{\xi}_1^H\} = N_0 \mathbf{F}_1$$

is the additive noise covariance matrix at the decorrelator output. In the above equation

$$\begin{aligned} \mathbf{F}_1 &= \text{diag}[F_1^{(b1)}, \dots, F_1^{(bK)}, F_1^{(b1)}, \dots, F_1^{(bK)}] \\ &= \text{diag}[\mathbf{F}_1(i), \mathbf{F}_1(i)] \end{aligned} \quad (10)$$

accounts for the noise enhancement in $2K$ blocks over symbols $(i-1)$ and i due to decorrelation, and $F_1^{(bj)} = (\mathbf{P}^{(bj)})_{1,1}^{-1}$, $j = 1, \dots, K$ is the $(1,1)^{st}$ element of the matrix $(\mathbf{P}^{(bj)})^{-1}$.

Because we assume that the fading process is wide-sense stationary and normalized, $\mathbf{R}_{\mathbf{c}_1}$ is Hermitian and positive semi-definite with diagonal elements equal to one.

The decorrelator output vector \mathbf{z}_1 , being the sum of two independent complex Gaussian random vectors (due to the Rayleigh type of fading), has a $2K$ -variate complex Gaussian distribution [15], [12]

$$p(\mathbf{z}_1) = \frac{1}{\pi^{2K} |\mathbf{R}_{\mathbf{z}_1}|} e^{-\mathbf{z}_1^H \mathbf{R}_{\mathbf{z}_1}^{-1} \mathbf{z}_1} \quad (11)$$

where $|\mathbf{R}_{\mathbf{z}_1}|$ is the determinant of $\mathbf{R}_{\mathbf{z}_1}$.

Let hypothesis “ H_1 ” correspond to the transmission of the information bit 1, i.e., of pairs of differentially encoded symbols $(-1, -1)$ or $(1, 1)$ over two consecutive symbol intervals, and let hypothesis “ H_0 ” correspond to the transmission of the information bit -1 . The likelihood ratio can be written as

$$\Lambda(\mathbf{z}_1) = \frac{p(\mathbf{z}_1|H_1)}{p(\mathbf{z}_1|H_0)} = \frac{\frac{1}{\pi^{2K} |\mathbf{R}_{\mathbf{z}_1(1)}|} e^{-\mathbf{z}_1^H \mathbf{R}_{\mathbf{z}_1(1)}^{-1} \mathbf{z}_1}}{\frac{1}{\pi^{2K} |\mathbf{R}_{\mathbf{z}_1(-1)}|} e^{-\mathbf{z}_1^H \mathbf{R}_{\mathbf{z}_1(-1)}^{-1} \mathbf{z}_1}} \quad (12)$$

where $\mathbf{R}_{\mathbf{z}_1(1)}$ and $\mathbf{R}_{\mathbf{z}_1(-1)}$ are the covariance matrices of \mathbf{z}_1 corresponding to the transmission of the information bits 1 and -1 , respectively. These covariance matrices can be written as

$$\begin{aligned} \mathbf{R}_{\mathbf{z}_1(1)} &= \mathcal{E}_1 \mathbf{R}_{\mathbf{c}_1} \mathcal{E}_1^H + \mathbf{R}_{\boldsymbol{\xi}_1} = \mathbf{R} \\ \mathbf{R}_{\mathbf{z}_1(-1)} &= (\mathcal{E}_1 \mathbf{R}_{\mathbf{c}_1} \mathcal{E}_1^H + \mathbf{R}_{\boldsymbol{\xi}_1}) \otimes \begin{bmatrix} \mathbf{1} & -\mathbf{1} \\ -\mathbf{1} & \mathbf{1} \end{bmatrix}. \end{aligned} \quad (13)$$

In (13), $\mathbf{1}$ is a $K \times K$ square matrix with all elements equal to 1, and \otimes stands for the Hadamard product, giving element by element multiplication. The maximum *a posteriori* (MAP) decision rule can be formulated as

$$\Lambda(\mathbf{z}_1) \underset{H_0}{\overset{H_1}{\geq}} \frac{\Pr(H_0)}{\Pr(H_1)}. \quad (14)$$

Assuming equally likely information bits, the determinant of $\mathbf{R}_{\mathbf{z}_1}$ does not depend on the sign of the transmitted bit. By taking the logarithm of both sides of (12), the decision statistics for the i th information bit can be expressed as

$$\lambda_i = \mathbf{z}_1^H (\mathbf{R}_{\mathbf{z}_1(-1)}^{-1} - \mathbf{R}_{\mathbf{z}_1(1)}^{-1}) \mathbf{z}_1 = \mathbf{z}_1^H \mathbf{Q} \mathbf{z}_1. \quad (15)$$

The decision rule, then, is

$$\lambda_i \begin{cases} > 0, & \text{decide “1”} \\ < 0, & \text{decide “-1”}. \end{cases}$$

It should be noted that an inversion of the $2K \times 2K$ matrix is required before performing the hypothesis test.

C. Error Performance Analysis

A transformation, as performed in [16] and [12], can also be performed on the quadratic form of the decision variable in (15). The details of the derivation are shown in the Appendix, where the decision variable in (A1) is reduced to a diagonal Hermitian form with independent variates. Specifically, there exists a linear transformation $\mathbf{w} = \mathbf{T} \mathbf{S}$, such that

$$\lambda_i = b_1(i) \mathbf{w}^H \boldsymbol{\Gamma} \mathbf{w} \quad (16)$$

where $\mathbf{w} = [w_1 \dots w_{2K}]^T$ is a complex Gaussian random vector with unit variance and independent elements, i.e., $E\{\mathbf{w} \mathbf{w}^H\} = \mathbf{I}$, with \mathbf{I} being the unit matrix, and

$$\boldsymbol{\Gamma} = \text{diag}[\gamma_1, \dots, \gamma_{2K}]$$

where γ_u , $u = 1, \dots, 2K$ are the eigenvalues of the $2K \times 2K$ matrix $\mathbf{R} \mathbf{Q}$. Denoting the nonzero eigenvalues of matrix $\mathbf{R} \mathbf{Q}$ as γ_u , $u = 1, \dots, M$, the characteristic function of the quadratic form in (16) for this case is

$$\psi_\lambda(j\omega) = \frac{1}{\det(\mathbf{I} - j\omega \boldsymbol{\Gamma})} = \prod_{u=1}^M \frac{1}{1 - j\omega \gamma_u} = \sum_{u=1}^M \frac{\beta_u}{1 - j\omega \gamma_u} \quad (17)$$

where β_u are the coefficients of the partial fraction expansion of $\psi_\lambda(j\omega)$, i.e.,

$$\beta_u = \prod_{\substack{v=1 \\ v \neq u}}^M \frac{\gamma_u}{\gamma_u - \gamma_v}.$$

In the case of distinct nonzero eigenvalues (which occurs in situations of practical interest), the probability of error of this quadratic form is given by [15], [17]

$$P_e = P\{\lambda_i < 0\} = \sum_{\gamma_u < 0} \beta_u = \sum_{\gamma_u < 0} \prod_{\substack{v=1 \\ v \neq u}}^M \frac{\gamma_u}{\gamma_u - \gamma_v}. \quad (18)$$

IV. NUMERICAL EXAMPLES AND DISCUSSION

As mentioned in Section III, the piecewise-constant representation of the fading process in each block of time exhibits nonuniformity along the time axis. For convenience, in our numerical examples, the blocks of time were chosen as integer multiples of the chip period T_c . For the first-order Markov fading model, the correlation parameter ρ' in the recursion $c_k((n+1)T_c) = \rho' c_k(nT_c) + \chi(nT_c)$, where $\chi(nT_c)$ is a zero-mean complex Gaussian random variable with the variance $1 - \rho'^2$, was modified as $\rho' = \rho^{T_c/T}$. The elements of the vector of channel coefficients \mathbf{C}_1 in (8), for this and for the Jakes model (which employs 16 sinusoids), are the values at the time instants corresponding to the users' relative delays.

We consider a three-user scenario with signature waveforms chosen from Gold sequences of length 31 assigned to each user. In the examples below, the relative delays are set at $\tau_1 = 0$, $\tau_2 = (3/31)T$, and $\tau_3 = (15/31)T$, resulting in the following value of the corresponding noise enhancement matrix in (10): $\mathbf{F}_1 = \text{diag}[1.5 \ 1.0345 \ 1.1852 \ 1.5 \ 1.0345 \ 1.1852]$. With the previous assumption of $E\{|c_k|^2\} = 1$, the signal-to-noise ratio (SNR) for user 1 is defined as $\text{SNR}_1 = a_1/N_0$.

Before presenting the performance results of the proposed detector, we note that we simulated the performance of the detector in [12] in a multiaccess environment under ideal power control. Using Jakes model with $f_d T = 0.08$, and the multiaccess parameters of the previous paragraph, we found that, due to multiaccess interference, the error floor reaches the value of about 10^{-1} , well above that of the conventional (symbol-spaced) detector in a single-user environment.

We compare the error performance of the proposed detector only to that of the conventional DPSK receiver in a single-user environment, which utilizes one sample per symbol. We do this because the latter, as shown in [10], has the same error floor as the infinite horizon decorrelator used in conjunction with the conventional differentially coherent detection, while at low SNR's, with the same values of input parameters given in our numerical examples, their performance curves are almost indistinguishable. Fig. 3 provides a performance comparison for the channel modeled by the first-order Markov process. The fading rates $f_d T = 0.04$ and $f_d T = 0.08$ in (3) were chosen, and for both fading rates the proposed detector demonstrates clear superiority by significantly lowering the error floor. In Fig. 4, the Jakes model with $f_d T = 0.08$ and $f_d T = 0.16$ in (4) was employed for the same SNR range used in the previous model, but the error floor did not appear. In both fading channel models, the theoretical curves, as much as it was feasible, are confirmed by simulation.

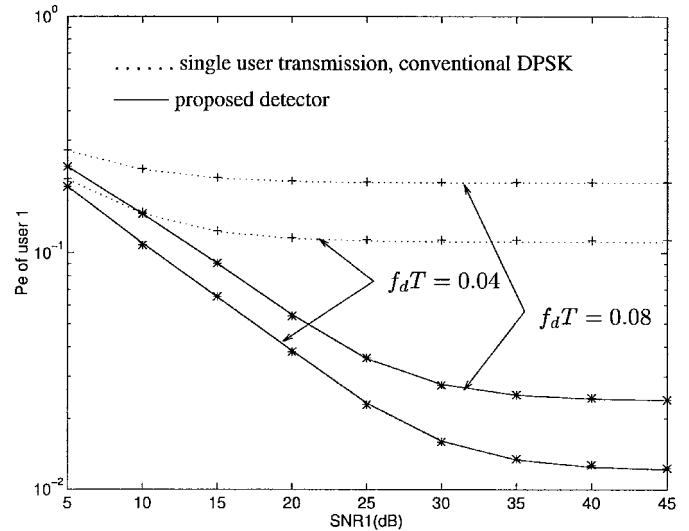


Fig. 3. Analytical and simulated (with marks) error performance curves with first-order Markov model.

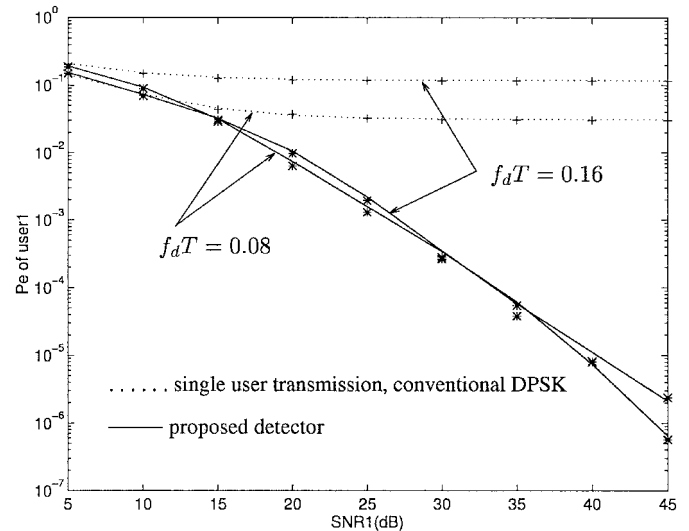


Fig. 4. Analytical and simulated (with marks) error performance curves with Jakes model.

To assess the reasons for the performance improvement achieved by the proposed detector, (16) is rewritten as

$$\lambda_i = b_1(i) \sum_{u=1}^M \gamma_u |w_u|^2 = b_1(i) \sum_{u=1}^M \gamma_u \alpha_u. \quad (19)$$

Because \mathbf{w} is a complex Gaussian random vector with independent elements $w_k, \alpha_k, k = 1, \dots, M$, are i.i.d. random variables that follow chi-square distribution. The form of (19) bears similarity to the analysis of a single-user diversity reception in nonselective Rayleigh fading [16, Ch. 11]. In the proposed scheme, the decision process involves $2K$ random variables, each corresponding to the same information bit, but with a lowered SNR in each block. For a fading process with $\rho < 1$ (i.e., one that is not completely correlated), the receiver's structure may be considered as one that explores a form of time diversity. One can also invoke the explanation for the performance improvement given in [12] wherein the receiver,

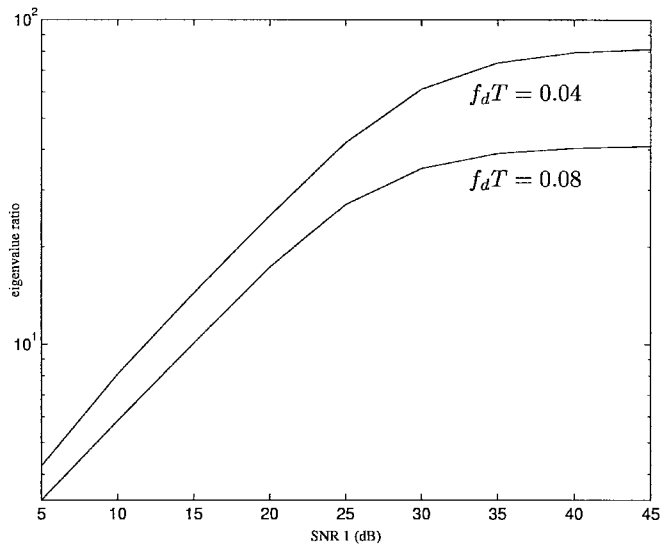


Fig. 5. Eigenvalue ratio curves with first-order Markov model.

by applying the ML principle to the fractionally sampled data, effectively increases the correlation in the fading process, resulting in a lowered error floor.

With the proposed detector, fractionally sampled matched filter outputs of the received multiuser signal are utilized for a dual benefit. Besides providing the basis for ML detection to lower the error floor, fractional sampling also provides the means for realizing a lower complexity bit-by-bit decorrelator, which requires inversion of $K \times K$ matrices only.

We note that the variation of the distribution of the users' relative delays do not appear to affect the performance when the Jakes model is used, while a much greater sensitivity results from the first-order Markov model. When the relative delays are very close to each other, there is a possibility that the correlation matrix for such a short block will become singular. Such a block can be excluded from consideration, for the remaining $K - 1$ blocks carrying the same information will be sufficient for performing a proper detection.

In the example in Fig. 4, the proposed detector does not exhibit the error floor within the specified range of SNR values.¹⁰ To provide an intuitive, yet quantitative explanation of the displayed behavior, we analyze the nonzero eigenvalues of matrix RQ , which depend, among other parameters, on the fading rate. It can be observed from (19) that if information bit $+1$ is transmitted, a decision error is made if the sum of the negative eigenvalues exceeds the sum of the positive ones. For the fading rates of interest, numerical examples suggest that there is a dominant positive eigenvalue for both fading models, and a dominant negative (in absolute value) eigenvalue for the first-order Markov model. Plots of the ratio of the absolute values of the largest positive and negative eigenvalues versus the SNR are shown in Figs. 5 and 7 for the same fading rates used in our numerical examples. The SNR value at which the eigenvalue ratio flattens out can serve as a rough estimate of the SNR value at which the probability of error curve

¹⁰ A higher value of $f_d T$, which would certainly cause the error floor to appear at more "reasonable" SNR values, would preclude obtaining matched filter outputs in the form given in (5).

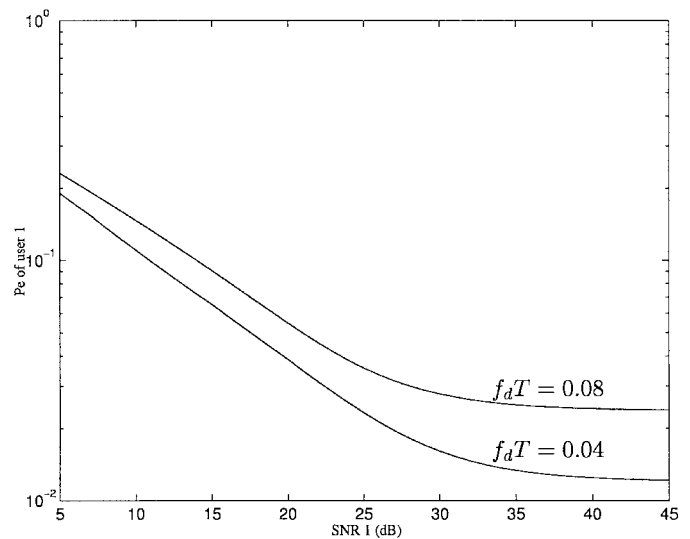


Fig. 6. Analytical error performance curves with first-order Markov model over wide range of SNR values.

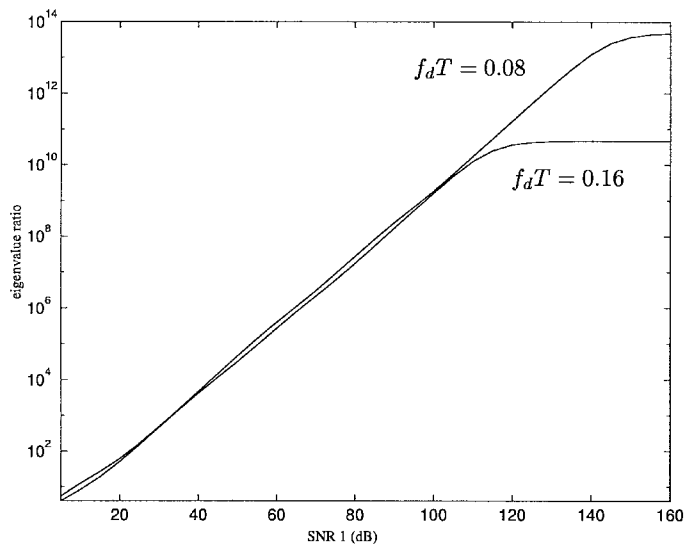


Fig. 7. Eigenvalue ratio curves with Jakes model.

does the same, i.e., where the error floor is exhibited. Figs. 6 and 8 show the corresponding analytical error performance curves for both models over a wide range of SNR values. The respective error floors for both fading rates appear at approximately 30 and 35 dB for the first-order Markov model, and at approximately 110 dB and 140 dB for Jakes' model, as suggested by Figs. 5 and 7.

V. CONCLUSION

A differentially coherent multiuser detector for a time-varying single path Rayleigh fading channel, which requires only the statistics but not the realization of the fading parameters, is proposed. The realization of the decorrelator, which in a K -user CDMA environment needs the inversion of $K \times K$ matrices only, is based on utilizing fractionally sampled matched filter outputs. Oversampling also provides the basis for the ML principle detection that results in an effective

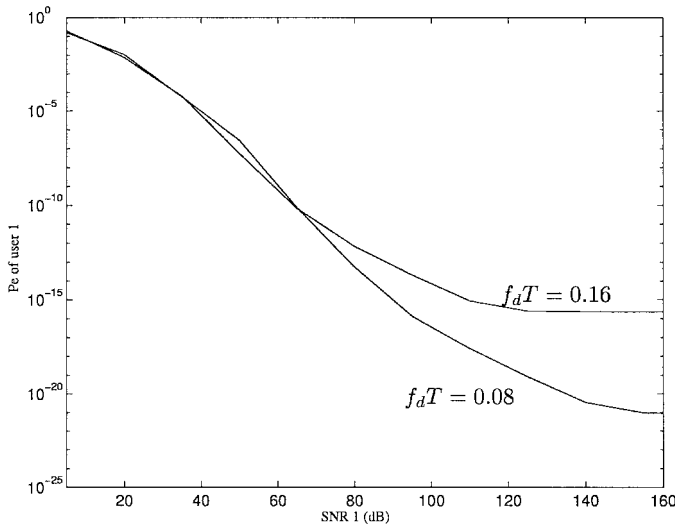


Fig. 8. Analytical error performance curves with Jakes model over wide range of SNR values.

increase of the correlation in the fading process, and, hence, significantly lowers the error floor. The error performance analyzed on two different fading channel models suggests significant improvement in terms of lowering the error floor in comparison to conventional differentially coherent detection.

APPENDIX

Considering the differentially encoded symbols $d_1(i-1)$ and $d_1(i)$ in the intervals $(i-1)$ and i , respectively, define

$$\mathbf{S} = \begin{bmatrix} \mathbf{S}(i-1) \\ \mathbf{S}(i) \end{bmatrix} = \begin{bmatrix} \sqrt{a_1} \mathbf{E}_1(i) \mathbf{C}_1(i-1) + \boldsymbol{\xi}_1(i-1) \\ \sqrt{a_1} \mathbf{E}_1(i) \mathbf{C}_1(i) + \boldsymbol{\xi}_1(i) \end{bmatrix}$$

which corresponds to the received signals of user 1 over the $(i-1)$ th and the i th bit intervals with transmitted differentially encoded bits $d_1(i-1)$ and $d_1(i)$ removed. Also defining

$$\mathbf{U} = E\{\mathbf{S}(i)\mathbf{S}(i)^H\}$$

a $K \times K$ matrix representing the correlation matrix over one bit interval, and

$$\mathbf{V} = E\{\mathbf{S}(i-1)\mathbf{S}(i)^H\}$$

a $K \times K$ matrix representing the cross-correlation matrix over adjacent bit intervals, matrix \mathbf{R} can be partitioned as

$$\begin{aligned} \mathbf{R} &= E\{\mathbf{S}\mathbf{S}^H\} \\ &= \begin{bmatrix} \mathbf{U} & \mathbf{V} \\ \mathbf{V}^H & \mathbf{U} \end{bmatrix}. \end{aligned}$$

The inverse of \mathbf{R} in (13) can be obtained by using a matrix inversion lemma as in [12].

The matrix \mathbf{Q} can be transformed into

$$\mathbf{Q} = \begin{bmatrix} \mathbf{0} & \boldsymbol{\Delta} \\ \boldsymbol{\Delta}^H & \mathbf{0} \end{bmatrix}$$

where $\mathbf{0}$ is a $K \times K$ matrix with all elements equal to zero and

$$\boldsymbol{\Delta} = 2\mathbf{U}^{-1}\mathbf{V}\boldsymbol{\Theta}^{-1}$$

and

$$\boldsymbol{\Theta} = \mathbf{U} - \mathbf{V}^H\mathbf{U}^{-1}\mathbf{V}.$$

It is easy to show that the decision variable in (15) is equivalent to

$$\begin{aligned} \lambda_i &= \mathbf{S}^H \begin{bmatrix} \mathbf{0} & \mathbf{D}_1(i-1)\mathbf{D}_1(i)\boldsymbol{\Delta} \\ \mathbf{D}_1(i-1)\mathbf{D}_1(i)\boldsymbol{\Delta}^H & \mathbf{0} \end{bmatrix} \mathbf{S} \\ &= b_1(i)\mathbf{S}^H \begin{bmatrix} \mathbf{0} & \boldsymbol{\Delta} \\ \boldsymbol{\Delta}^H & \mathbf{0} \end{bmatrix} \mathbf{S} \end{aligned} \quad (\text{A1})$$

where $b_1(i) = d_1(i-1)d_1(i) \in [-1, 1]$ is the i th information bit before differential encoding.

We can then transform \mathbf{S} , whose elements of signal part are correlated with each other, into another complex Gaussian random vector with unit variance and independent elements using a linear transformation.

ACKNOWLEDGMENT

This work was performed while the authors were with New Jersey Institute of Technology, Newark, NJ USA.

REFERENCES

- [1] S. Verdú, "Minimum probability of error for asynchronous Gaussian multiple-access channels," *IEEE Trans. Inform. Theory*, vol. IT-32, pp. 85–96, Jan. 1986.
- [2] R. Lupas and S. Verdú, "Linear multiuser detectors for synchronous code-division multiple-access channels," *IEEE Trans. Inform. Theory*, vol. 35, pp. 123–136, Jan. 1989.
- [3] S. Verdú, "Recent progress in multiuser detection," in *Advances in Communications and Signal Processing*. New York: Springer-Verlag, 1989, pp. 27–38.
- [4] ———, "Adaptive multiuser detection," in *Code Division Multiple Access Communications*. Kluwer Academic Publishers, 1995, pp. 97–115.
- [5] A. Duel-Hallen, J. Holtzman, and Z. Zvonar, "Multiuser detection for CDMA systems," *IEEE Personal Commun.*, vol. 2, pp. 46–58, Apr. 1995.
- [6] S. Vasudevan and M. K. Varanasi, "Receivers for CDMA communication over time-varying Rayleigh fading channels," *Proc. Communication Theory Mini-Conf., Globecom 1993*, Houston, TX, Nov. 1993, pp. 60–64.
- [7] H. Y. Wu and A. Duel-Hallen, "Multiuser detection with differentially encoded data for mismatched flat Rayleigh fading CDMA channels," *Proc. 1996 Conf. on Information Sciences and Systems*, Princeton, NJ, Mar. 1996, pp. 332–337.
- [8] M. K. Varanasi, "Noncoherent detection in asynchronous multiuser channels," *IEEE Trans. Inform. Theory*, vol. 39, pp. 157–176, Jan. 1993.
- [9] Z. Zvonar and D. Brady, "Differentially coherent multiuser detection in asynchronous CDMA flat Rayleigh fading channels," *IEEE Trans. Commun.*, vol. 43, pp. 1252–1255, Feb./Mar./Apr. 1995.
- [10] ———, "Adaptive multiuser receivers with diversity reception for nonselective Rayleigh fading asynchronous CDMA channels," in *Proc. IEEE Military Communications Conference*, Fort. Monmouth, NJ, Oct. 1994, pp. 982–986.
- [11] L. Zhong and Z. Siveski, "A parallel one-shot decorrelator structure for asynchronous multiuser AWGN channel," *Proc. 1995 Conf. on Information Sciences and Systems*, Baltimore, MD, Mar. 1995, pp. 205–208.
- [12] W. Dam and D. Taylor, "An adaptive maximum likelihood receiver for correlated Rayleigh-fading channels," *IEEE Trans. Communications*, vol. 42, pp. 2684–2692, Sept. 1994.
- [13] J. G. Proakis, *Digital Communications*, 3rd ed., New York: McGraw-Hill, 1995.
- [14] W. C. Jakes, *Microwave Mobile Communications*. New York: Wiley, 1974.
- [15] M. Barrett, "Error probability for optimal and suboptimal quadratic receivers in rapid Rayleigh fading channels," *IEEE J. Select. Areas Commun.*, vol. SAC-5, pp. 302–304, Feb. 1987.
- [16] M. Schwartz, W. R. Bennett, and S. Stein, *Communication Systems and Techniques, Chapter 10*. New York: McGraw-Hill, 1966.
- [17] Z. Zvonar, "Multiuser detection for Rayleigh fading channels," Ph.D. dissertation, Northeastern Univ., Boston, MA, 1993.



Huaping Liu received the B.S. and M.S. degrees from Nanjing University of Posts and Telecommunications, Nanjing, China, in 1987 and 1990, respectively, and the Ph.D. degree from New Jersey Institute of Technology (NJIT), Newark, NJ, in 1997, all in electrical engineering.

He is currently a Member of Technical Staff in the Wireless Networks Group, Lucent Technologies, Whippany, NJ. His research interest is in wireless CDMA systems.

Dr. Liu received the Hashimoto Prize by NJIT for his doctoral research.



Zoran Siveski (S'83–M'89) received the Dipl.Ing. degree from the University of Belgrade and the Ph.D. degree from the City University of New York, both in electrical engineering.

He is currently a Member of Technical Staff in the Wireless Networks Group, Lucent Technologies, Whippany, NJ, and is involved in the performance analysis for wireless access technologies.